PHYSICAL REVIEW C VOLUME 46, NUMBER 4 OCTOBER 1992

Shape coexistence and extreme deformations near A=80

J. P. Maharana and Y. K. Gambhir
Department of Physics, Indian Institute Of Technology, Bombay 400 076, India

J. A. Sheikh
Tata Institute of Fundamental Research, Bombay 400 005, India

P. Ring
Physik-Department der Technischen Universität München, D-8046 Garching, Federal Republic of Germany

(Received 2 March 1992)

The neutron deficient Sr and Zr nuclei are studied in the relativistic mean-field approach. Large deformations and shape coexistence are predicted for these nuclei in the vicinity of the proton drip line. The charge radii are found to increase with the removal of neutrons from the semimagic ^{88}Sr and ^{90}Zr, in close agreement with the recent isotopic-shift measurements.

PACS number(s): 21.60.Jz, 21.60.Ev, 21.10.−k, 27.50.+e

Isomerism between different possible shapes is well recognized in nuclear spectroscopy. This phenomenon is related to the population patterns of protons and neutrons around the fermi surface. For instance, in the mercury region the shape isomerism exists between small oblate and large prolate deformed structures [1]. The former is caused by an almost closed proton shell and the latter one by an open neutron shell. A similar situation occurs in the mass-120 region where protons occupy the lower half of the $1h_{11/2}$, driving the system to prolate shape, and the neutrons occupying the upper half of the $1h_{11/2}$ leading to the oblate deformation. The coexistence of these two shapes leads to the occurrence of two S bands corresponding to the two structures.

Shape isomerism is also possible between spherical and deformed structures. One of the early experiments [2] to identify this possibility was in ^{72}Se. This kind of shape coexistence is possible with the intruder orbital (giving rise to deformation) appearing among the natural parity states. In the mass-80 region the intruder orbital $1g_{9/2}$ is near to $1p_{1/2}$. In the present work we have studied some of the nuclei in this region to explore the possibility for shape coexistence in the framework of the relativistic mean-field (RMF) theory [3, 4]. This RMF approach has been found to be very successful [4] in correlating the measured nuclear ground state properties throughout the mass table. The RMF framework starts with a Lagrangian density containing the nucleonic and mesonic degrees of freedom and the so-called set of RMF equations are derived from the variational procedure which are then solved self-consistently. Here the mesons considered are (i) scalar sigma $\sigma(J^\pi = 0^+, T = 0)$, (ii) vector omega $\omega(J^\pi = 1^-, T = 0)$, (iii) isovector vector rho $\rho(J^\pi = 1^-, T = 1)$. The pi (π) meson does not contribute in the present RMF (relativistic Hartree) approach for the nuclear states having a definite parity. The Lagrangian density with these mesons is then written as

$$\begin{aligned} L = {} & \bar{\psi}_i \left(i\gamma^\mu \partial_\mu - M\right) \psi_i + \tfrac{1}{2}\partial^\mu \sigma \partial_\mu \sigma - U(\sigma) - g_\sigma \bar{\psi}_i \psi_i \sigma \\ & - \tfrac{1}{4}\Omega^{\mu\nu}\Omega_{\mu\nu} + \tfrac{1}{2} m_\omega^2 \omega^\mu \omega_\mu - g_\omega \bar{\psi}_i \gamma^\mu \psi_i \omega_\mu \\ & - \tfrac{1}{4}\mathbf{R}^{\mu\nu}\mathbf{R}_{\mu\nu} + \tfrac{1}{2} m_\rho^2 \boldsymbol{\rho}^\mu \boldsymbol{\rho}_\mu - g_\rho \bar{\psi}_i \gamma^\mu \boldsymbol{\tau} \psi_i \boldsymbol{\rho}_\mu \\ & - \tfrac{1}{4} F^{\mu\nu} F_{\mu\nu} - e\bar{\psi}_i \gamma^\mu \frac{(1-\tau_3)}{2} \psi_i A_\mu, \end{aligned} \tag{1}$$

the sigma (σ) meson is assumed to move in a nonlinear potential [5]

$$U(\sigma) = \tfrac{1}{2} m_\sigma \sigma^2 + \tfrac{1}{3} g_2 \sigma^3 + \tfrac{1}{4} g_3 \sigma^4. \tag{2}$$

The standard sum convention is used for index "i" in Eq. (1) and runs over all the nucleons (A) represented by the Dirac spinors ψ_i with the bare mass M. Isovector quantities are indicated by the bold-faced letters. Here m_σ, m_ω, and m_ρ are the $\sigma-$, $\omega-$, and $\rho-$ meson masses, respectively, and $g_\sigma, g_\omega, g_\rho$ and $\frac{e^2}{4\pi} = \frac{1}{137}$ represent the corresponding coupling constants for the mesons and for the photon. The $\Omega^{\mu\nu}$, $\mathbf{R}^{\mu\nu}$, and $F^{\mu\nu}$ are the field tensors for the vector mesons and for the photon (Ref. [4]).

The variational principle for the static case along with the time reversal invariance and charge conservation leads to the Dirac equation for the nucleons with Lorentz scalar and the timelike component vector potentials and the Klein-Gordon type equations for the mesons and for the photon having source terms. These so-called RMF equations are to be solved self-consistently. For this we use the expansion technique developed in Ref. [4] and expand the Dirac and Klein-Gordon solutions into the deformed harmonic oscillator basis with frequency $\hbar\omega = 41A^{-1/3}$ and the deformation parameter (β_0). The number of oscillator major shells used in the expansions for the Dirac spinors (meson) fields are $N_F(N_B) = 12$ for the deformed solutions and $N_F(N_B) = 20$ with $\beta_0 = 0.0$ for the spherical solutions (for details see Ref. [4]). We have checked the convergence of the results with respect

to this basis truncation. It turns out that the calculations with $N_F = 8$ yield for ^{80}Zr about 3.5 MeV less binding and a larger quadrupole moment ($\sim$ 10%) as compared to the calculations with $N_F = 10$ or 12. The results with $N_F = 10$ and 12 are very similar, where the energy difference is of the order of 0.6 MeV and the difference in deformation is less than 3%. For the spherical case the energy difference is 0.2 MeV and the change in the charge radius is less than 0.3% for the case of $N_F = 12$ and 20 shells. Therefore $N_F \geq 10$ is required for accurate results. The results are not so sensitive on N_B and a value greater than or equal to 8 is sufficient.

The parameters appearing in the Lagrangian are taken from the earlier work [4, 6] and correspond to the nonlinear set NL1, a very successful set for the entire periodic table. The explicit values of these parameters are the masses (MeV) $M = 938.0$, $m_\sigma = 492.25$, $m_\omega = 795.359$, $m_\rho = 763.0$; and the coupling constants g_σ=10.138, g_ω=13.285, g_ρ=4.9755, g_2=-12.172, g_3=-36.265. The pairing which is important for the open shell nuclei is taken into account in a constant gap approximation [7]. The gap parameters Δ_n (Δ_p) for neutrons (protons) required in the calculations are taken from the observed odd-even mass difference [8] wherever available, otherwise estimated through the empirical relation Δ_n (Δ_p) $= \frac{12}{N^{1/2}(Z^{1/2})}$. The gaps obtained from this relation are found to be very close to those obtained from various theoretical mass tables, e.g., Moller and Nix listed in Ref. [9]. It is found that the sensitivity of the calculated results on the explicit values of the gap parameters is rather small. For example, the decrease in both Δ_n and Δ_p from the initial 1.9 MeV to 1.5 MeV decreases the total calculated binding energy of ^{80}Zr by about 0.8 MeV both for the spherical and for the deformed solutions while the quadrupole moment changes by about 5% and the charge radius is almost unaffected.

The numerical calculations have been carried out for $^{74-88}$Sr and $^{76-90}$Zr nuclei. The calculations yield the total binding energy (E), the single particle energies, proton (neutron) intrinsic quadrupole moments Q_p (Q_n) and the corresponding hexadecupole moments, the point proton and neutron rms radii r_p (r_n) from which one can obtain the total rms radii. Some of the relevant quantities are given in Table I for the representative nuclei. Table I also includes the charge radius r_c and the deformation parameter β obtained through the following relations:

$$r_c = (r_p^2 + 0.64)^{1/2},$$
$$\beta = \sqrt{\frac{5}{16\pi}}\frac{4\pi}{3}\frac{1}{AR_0^2}(Q_n + Q_p), \tag{3}$$

where $R_0 = 1.2A^{1/3}$. The hexadecupole moments are not given in Table I since they were found to be quite small for all the studied nuclei. The second and third columns give the binding energies corresponding to the spherical (Sph.) and the deformed (Def.) solutions. For even nuclei $^{74-80}$Sr, $^{76-82}$Zr two solutions were obtained which are very close on the energy scale. The deformed solutions correspond to very large deformations with β values exceeding 0.4. These large deformation values are close to those of the superdeformed shapes. Of course for a quantitative comparison with the experimental values the deformed solution has to be mixed with the spherical solution since the two solutions coexist. The obtained binding energies are compared with the measured values wherever available or with the theoretical values of Moller and Nix labeled MN. The binding energies obtained in the present work are seen to be in good agreement with these values. For even $^{82-88}$Sr and $^{84-90}$Zr only the results for the spherical case are presented; the deformed solution, if it exists, probably lies much higher in energy. The nuclei with N=42 (^{80}Sr,^{82}Zr) appear to be transitional with more separation between the deformed and the spherical solutions as compared to the more neutron deficient nuclei. It is to be added here that the binding

TABLE I. Results of the relativistic mean-field (RMF) calculations: binding energies E (in MeV), charge radii r_c and root mean square radii rms (in fm), point proton quadrupole moments Q_p (in barns), and the deformation parameter β. The entries designated by MN correspond to the values extracted from the tables of Moller and Nix [13]. The obtained E in the present work are indeed very close to the experimental values wherever available [8].

A	E			r_c		rms		Q_p		β
	Sph.	Def.	MN	Sph.	Def.	Sph.	Def.	RMF	MN	RMF
^{74}Sr	–608.36	–608.69	–608.70	4.33	4.31	4.15	4.17	3.26	2.9	0.43
^{76}Sr	–637.76	–638.12	–637.90	4.31	4.32	4.16	4.20	3.52	3.2	0.46
^{78}Sr	–665.17	–663.59	–663.49	4.29	4.31	4.18	4.23	3.52	3.2	0.46
^{80}Sr	–688.70	–686.06	–686.17	4.28	4.30	4.21	4.24	3.21	3.2	0.41
^{82}Sr	–710.54		–708.12	4.29		4.24				
^{88}Sr	–768.12		–768.13	4.25		4.29				
^{76}Zr	–610.57	–609.12	–607.86	4.41	4.38	4.20	4.22	3.51	3.2	0.43
^{78}Zr	–642.42	–640.97	–639.32	4.39	4.39	4.21	4.25	3.80	3.5	0.47
^{80}Zr	–672.14	–669.04	–668.47	4.37	4.38	4.23	4.27	3.86	3.6	0.47
^{82}Zr	–697.95	–693.68	–694.15	4.35	4.36	4.24	4.27	3.47	–1.4	0.41
^{84}Zr	–721.21		–719.47	4.34		4.26				
^{90}Zr	–785.63		–784.00	4.30		4.29				

energies could be improved upon by readjusting the value of the parameter g_ρ. For example, the calculated binding energies can be brought almost in perfect agreement with the experimental values by using the value 5.250 instead of 4.9755 for g_ρ. It is to be added here that this change in g_ρ hardly affects the other properties.

Experimentally ^{76}Sr and ^{80}Zr have been populated [10]. It does appear that the ground state deformation for these nuclei is very large. The large deformations and the other properties of the nuclei in this region have been fairly understood in the various nonrelativistic mean-field theories and their extensions [11–15]. The reason for this strongly deformed shape obtained for these nuclei is due to the population of the $1g_{9/2}$ orbital. This has been revealed for the case of ^{80}Zr through the recent density-dependent Hartree-Fock (DDHF) with the Skyrme-type interaction [14] and from the conventional HF-band mixing [15] calculations. In the former the energy difference ΔE between the spherical and the deformed 12p-12h (6 protons and 6 neutrons in $1g_{9/2}$ shell) is found to be around 0.5, 3.4, and 2.2 MeV depending upon the kind of interaction Sk2, Sk3, and Sk3 with pairing, respectively, used in the calculations. In the latter the intrinsic states are generated by the tagged HF (fixed occupancies) calculations with the modified Kuo-Brown interaction and assuming ^{56}Ni as the inert core. The calculated ΔE is about 3 MeV in this case. In addition, the solutions corresponding to 4p-4h, 6p-6h, and 8p-8h are found to lie lower than the 12p-12h solutions.

We have analyzed here the structures of the two solutions. It is found that $N = Z = 28$ forms almost a closed core (more than 99% occupied). The population of various valence orbitals above this closed core is shown in Fig. 1. In the case of the spherical solution the $1g_{9/2}$ orbital is almost empty and the $N = 40$, $Z = 40$ is almost filled thereby leading to a spherical shape. In the case of the deformed solution it is seen that the low-m orbitals of the $1g_{9/2}$ subshell are now occupied at the expense of the orbitals below (mainly from $f_{5/2}$ and $p_{1/2}$) $N = 40$, $Z = 40$. This population pattern is consistent with the generator coordinate method (GCM) using HF+BCS [13]. This population of the low-m orbitals of the high-j intruder subshell corresponds to a deformed shape with a larger quadrupole moment. This deformed solution approximately corresponds to 12p-12h (6 protons and 6 neutrons in $1g_{9/2}$ subshell) and is in agreement with the earlier calculations.

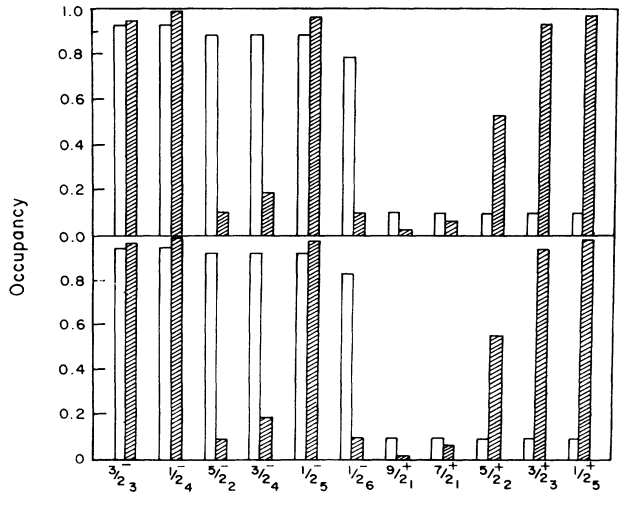

FIG. 1. The occupancies of the valence orbitals ($2p_{3/2}$, $1f_{5/2}$, $2p_{1/2}$, and $1g_{9/2}$) are plotted for neutrons (upper portion) and protons (lower half) for the case of ^{80}Zr. The empty blocks correspond to the spherical solution and the marked ones belong to the deformed solution.

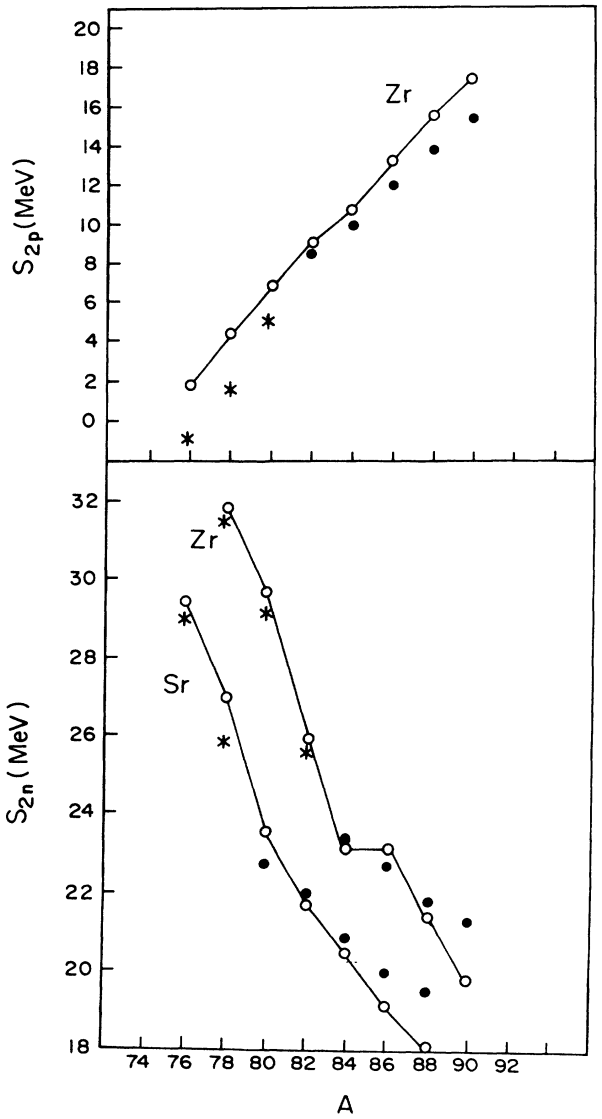

FIG. 2. The calculated two particle proton (neutron) separation energies S_{2p} (S_{2n}) (open circles) are plotted along with the experimental (solid circles) wherever available, otherwise with the extracted values from Moller and Nix (Ref. [9]) marked with an asterisk.

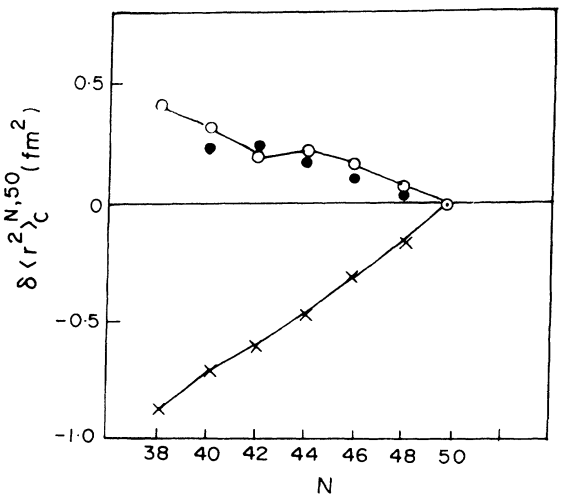

FIG. 3. The calculated differences in the charge root mean square radii with respect to ^{88}Sr (open circles) for the Sr isotopes are compared with the corresponding experimental values (Refs. [14] and [15]) shown by solid circles and with the density-dependent Hartree-Fock calculations (Ref. [16]) marked by crosses.

The calculated two-neutron (S_{2n}) and two-proton (S_{2p}) separation energies are shown in Fig. 2 along with those obtained from the observed masses wherever available [8], otherwise extracted from the calculations of Moller and Nix [16]. It is seen from Fig. 2 that the separation energies are indeed reproduced quite well in the present work.

The calculated charge radii are found to increase as more and more neutrons are removed from ^{88}Sr(^{90}Zr). In order to make it more transparent we plot $\delta < r^2 >_c^{N,50}$ the differences in charge square radius with respect to ^{88}Sr ($N = 50$) in Fig. 3 along with the recent isotopic shift measurements [17, 18] and the nonrelativistic density-dependent Hartree-Fock calculations [19]. It is evident from the figure that RMF reproduces the experimental data surprisingly well while DDHF fails and in fact produces the opposite trend. More recent calculations with GCM using HF+BCS substantially improve the situation, however the differences with the experiment remain [13].

From the present study it is possible to draw the following inferences.

(a) For the Sr and Zr isotopes close to the proton drip line two coexisting solutions were obtained, one with a very large deformation and other corresponding to a spherical shape. The deformations were found to be close to those of superdeformed shapes.

(b) The calculated binding energies and the two-particle separation energies were found to be in agreement with the measured values wherever available.

(c) The charge radii tend to increase with the removal of neutrons from the semimagic ^{88}Sr and ^{90}Zr cores and are found to be in close agreement with the isotopic shift measurements.

[1] D. Proetel, R.M. Diamond, P. Kienle, J.R. Leigh, K.H. Maier, and F.S. Stephens, Phys. Rev. Lett. **31**, 896 (1973).
[2] J.H. Hamilton, A.V. Ramayya, W.T. Pinkston, R.M. Ronningen, G. Garcia Bermudez, H.K. Carter, R.L. Robinson, H.J. Kim, and R.O. Sayer, Phys. Rev. Lett. **32**, 239 (1974).
[3] B.D. Serot and J.D. Walecka, Adv. Nucl. Phys. **198**, 1 (1986).
[4] Y.K. Gambhir, P. Ring, and A. Thimet, Ann. Phys. (N.Y.) **198**, 132 (1990), and references cited therein.
[5] J. Boguta and A.R. Bodmer, Nucl. Phys. **A292**, 413 (1977).
[6] P.G. Reinhard, M. Rufa, J. Maruhn, W. Greiner, and J. Friedrich, Z. Phys. A **323**, 13 (1986).
[7] P. Ring and P. Schuck, *The Nuclear Many-Body Problem* (Springer-Verlag, Berlin, 1980).
[8] A.H. Wapstra and G. Audi, Nucl. Phys. **A432**, 1 (1985).
[9] A.H. Wapstra, G. Audi, and R. Hoekstra, At. Data Nucl. Data Tables **39**, 281 (1988).
[10] C.J. Lister *et al.*, Phys. Rev. Lett. **59**, 1270 (1987).
[11] S. Åberg, H. Flocard, and W. Nazarewicz, Annu. Rev. Nucl. Part. Sci. **40**, 439 (1990).
[12] H. Flocard, in *Nuclear Structure of the Zirconium Region*, Proceedings of the International Workshop, Bad Honeff, 1988, edited by J. Ebert, R.A. Meyer, and K. Sistemich (Springer-Verlag, Berlin, 1988), p. 143.
[13] P. Bonche, J. Dobaczewski, H. Flocard, and P.H. Heenen, Nucl. Phys. **A530**, 149 (1991).
[14] D.C. Zheng and L. Zamick, Phys. Lett. B **266**, 5 (1991).
[15] R. Sahu and S.P. Pandya, J. Phys. G **14**, L165 (1988); **16**, 429 (1990).
[16] P. Moller and J.R. Nix, At. Data Nucl. Data Tables **26**, 165 (1981).
[17] D.A. Eastham *et al.*, Phys. Rev. C **36**, 1583 (1987).
[18] R.F. Silverans *et al.*, Phys. Rev. Lett. **60**, 2607 (1988).
[19] X. Campi and M. Epherse, Phys. Rev. C **22**, 2605 (1980).